JOURNAL OF MATERIALS SCIENCE **37** (2002) 1777–1783

Notched strength of satin-woven Si-Ti-C-O fiber-bonded ceramic composite

K. MATSUNAGA, T. ISHIKAWA, S. KAJII, T. HOGAMI, M. SATO
Ube Research Laboratiry, Ube industries Ltd, Ube City, Yamaguchi Prefecture, 755-8633, Japan
E-mail: 27500u@ube-ind.co.jp

S. OCHIAI
Mesoscopic Mat. Res. Center, Kyoto University, Sakyo-ku, Kyoto, 606-8501, Japan

The fracture behavior of Si-Ti-C-O fiber-bonded ceramic composite produced by hot-pressing oxidized 8 harness-satin-woven Si-Ti-C-O fibers was investigated by using unnotched and double edge notched tensile test specimens with different width (8 and 40 mm). The main results are summarized as follows. (i) The tensile strength of unnotched specimens for 8 mm width was higher than that for 40 mm width. Such a width-dependence of the unnotched strength could be described fairly well from the viewpoint of effective volume by application of the experimentally estimated Weibull's shape parameter. (ii) The applicability of the fracture toughness criterion (fracture arises when the stress intensity factor reaches the critical value) and net section stress criterion (fracture arises when the strength of the ligament reaches the unnotched strength) to the present composite was examined. The fracture strength of a notched specimen for 8 mm width was described by the net stress criterion. On the other hand, the strength for 40 mm width obeyed the net stress criterion for a small notch length but it shifted toward the fracture toughness criterion for large one. The shift of the fracture criterion from net strength- to fracture toughness-criterion arose around at the relative notch length 0.2 (notch length 8 mm), corresponding to periodical spacing of fiber strands (8 harness). (iii) The fiber pull-out length (0.4 mm on an average) was nearly the same as the half length of the fiber strand whose deformation is not constricted by the other strands in the satin-weave. (iv) The present fiber-bonded ceramic composite is insensitive to notch under the condition where the width of specimen is narrow and the notch length is smaller than 8 mm. This composite could be therefore applicable to industrial objects safely when the objects are designed as to satisfy the notch-insensitive condition.

1. Introduction

Development of the thermostructural materials, which withstand long-term use in corrosive environments at high temperatures, has been requested to achieve higher energy efficiency and additional functionality in the fields such as aerospace and power generation. Ceramic matrix composites (CMCs) reinforced with continuous fibers have been identified as the most promising candidate for such thermostructural materials, because they guarantee a high heat-resistance and an excellent fracture resistance [1–3].

Si-Ti-C-O fiber-bonded ceramic (Tyrannohex®) composite is produced by hot-press of the sheets or fabrics of a pre-oxidized Si-Ti-C-O fiber with the oxide layer of several hundred nano-meters in thickness. The structure of this composite is approximately similar to ordinary CMCs with an exception that the volume fraction of fiber is so high as around 87% [4]. This composite is one of the most promising candidates of thermostructural materials, since the strength can be retained even at 1400°C in air under the condition of holding time 600 s [5]. Moreover, as this composite has a lower thermal conductivity (1/10 of stainless steel), it is being developed also as the insulating material [6]. In the previous studies, the authors have investigated the microstructure and the mechanical properties of Si-Ti-C-O fiber-bonded ceramic composite [5–10], and have revealed the relations of fiber volume fraction, fiber orientation and so on to the unnotched strength. For practical application of this composite, further study on fracture behavior of notched specimens is needed.

Concerning the notched strength of CMCs and carbon fiber reinforced carbon composite (C/C composite), it has been one of the objectives of study to clarify which of the fracture toughness criterion (specimen is fractured when the stress intensity factor reaches a critical value) and the net stress criterion (specimen is fractured when the ligament portion reaches the unnotched strength) is applicable. It has been shown

experimentally that the fracture criterion of plain-woven C/C composite tends to shift from the net stress criterion toward the fracture toughness one with increasing ligament length when the interface is relatively strong [11]. Concerning the fracture criterion of Si-Ti-C-O fiber-bonded ceramic composite, only a few studies have so far been carried out until now. Only the result, indicating that the strength of unidirectional material can be described by the net stress criterion, has been reported [12].

In this work, the fracture strength of satin-woven fiber-bonded ceramic composites was studied by using unnotched and double edge notched tensile test specimens of two different widths (8 and 40 mm) to clarify the fracture criterion and the mechanism.

2. Experimental procedure

The reinforcing material used in this study was eight-harness satin weave fabric of Si-Ti-C-O fibers (Tyranno fiber®, LoxM grade, Ube Industries LTD.) containing oxygen of 12 mass %. Before fabrication of the preform, the bundles of fibers were oxidized in ambient air at 1000°C [8], and the satin weave fabrics of the pre-oxidized Si-Ti-C-O fibers, being covered with oxide layer on the surface, were prepared. A preform was then prepared by laminating the pre-oxidized satin weaves of Si-Ti-C-O fiber. Finally, the Si-Ti-C-O fiber-bonded ceramic composite was produced by hot-press of the preform in an argon atmosphere at 1750°C under a pressure of 40 MPa. The very little porosity was confirmed by scanning electron microscopy (see in Fig. 1a). The fiber with an average diameter of 8 μm was amorphous before production of the Si-Ti-C-O fiber-bonded ceramic composite. After production of the composite,

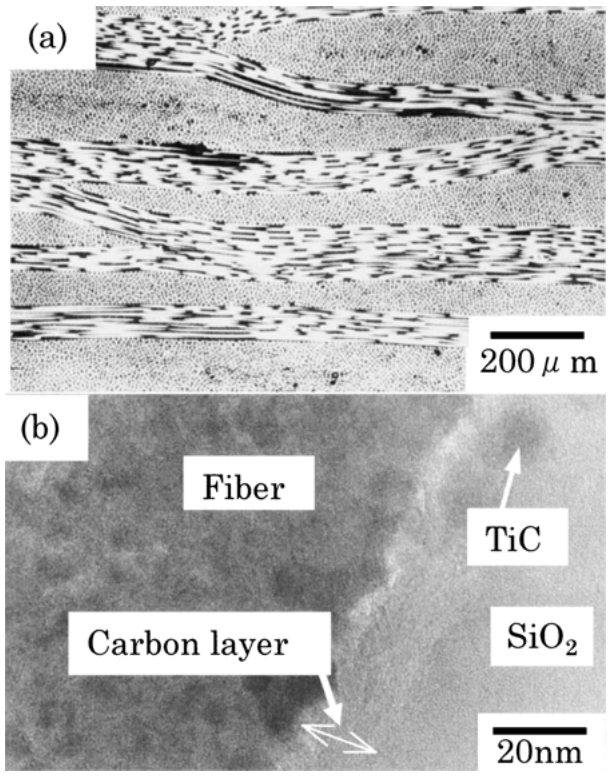

Figure 1 Optical micrograph of a cross section of Satin-Tyrannohex fabricated by the hot-press in argon atmosphere at 1750°C under 40 MPa.

TABLE I Typical properties of the present Si-Ti-C-O fiber-bonded ceramic composite

Chemical composition		$Si_1Ti_{0.03}C_{1.4}O_{0.44}$
Fiber content	(volume%)	87
Density	(g/cm^3)	2.46
Porosity	(%)	<1
Thermal expansion coefficient	(10^{-6}/°C)	3.1 (In plane)
Specific heat	J/kg°C	709
Thermal conductivity	(W/m°C)	3.29 (Room temperature)
Specific resistance	ohm · cm	0.1–0.5

TABLE II The test condition and relative notch length ($2a/W$)

Test temperature	W/mm	Relative notch length, $2a/W$
Room temperature	8	0.2, 0.3, 0.4, 0.6, 0.8
	40	0.2, 0.4, 0.6
1400°C	8	0.2, 0.4, 0.6

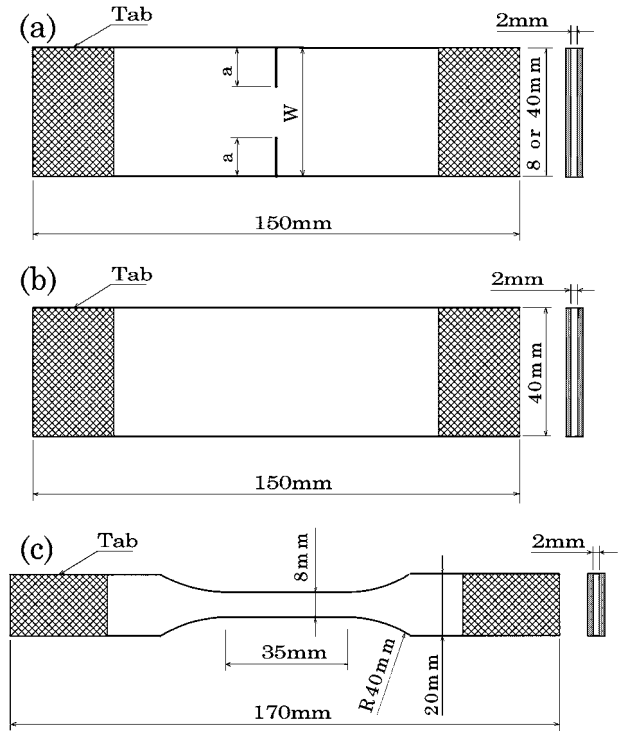

Figure 2 Shapes and dimensions of (a) notched and (b, c) unnotched specimens with 40(b) and 8 mm (c) widths.

the mixed structure of grown SiC crystals, amorphous SiO_2-based phase and turbostratic carbon layer were observed, as shown in Fig. 1b, similarly as in our former work [10]. Typical properties of the present Si-Ti-C-O fiber-bonded ceramic composite are listed in Table I.

The fracture strength of notched specimen was measured using the double edge notched tensile test specimens shown in Fig. 2a. The test condition and relative notch length ($2a/W$) are listed in Table II. The notch was introduced first with a slicing machine with a 0.5 mm width to the prescribed depth and then the tip radius was made to be about 50 μm on handicraft using a precision file. As reference specimens, unnotched specimens of two different widths (8 and 40 mm) were also prepared as shown in Fig. 2b and c.

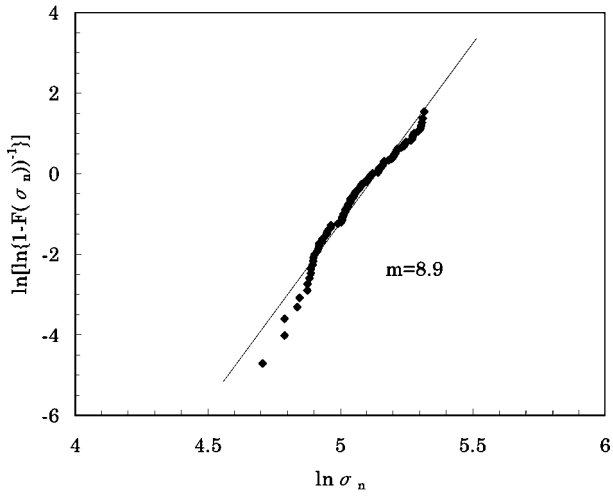

Figure 3 Weibull plot of the measured unnotched strength for 8 mm-width specimens. The solid line shows the result of fitting of the experimental data.

Tensile tests were performed at a crosshead speed of $0.5\ \text{mm} \cdot \text{min}^{-1}$ in air at room temperature and in argon atmosphere at 1400°C after a holding time of 600 s. The Weibull's shape and scale parameters [13] were estimated from the measured distribution of unnocthed strength of 102 specimens with 8 mm width. The estimated parameters were used to examine whether the difference in unnotched strength between 8 and 40 mm width-specimens can be described by the volume effect or not.

The morphology of the fracture surfaces was examined with a scanning electron microscope*(SEM) at an acceleration voltage of 10 kV. The pull-out length of fiber was measured from the fracture surface.

3. Result and discussion

3.1. Fracture behavior of notched specimen

Average tensile strength of unnotched specimens for 40 mm width was 119 MPa, whereas that for 8 mm width was 145 MPa. Evidently, the unnotched strength for 8 mm width was higher than that for 40 mm width. The reason for this is discussed below from the viewpoint of effective volume by applying the two parameter Weibull distribution function [13]. Fig. 3 shows the Weibull plot (plot of $\ln\ln(1-F)^{-1}$ against $\ln(\sigma_n)$ where F is the cumulative probability and σ_n the measured unnotched strength of the specimens with 8 mm width). The linearity between $\ln\ln(1-F)^{-1}$ and $\log(\sigma_n)$ is fairly good, indicating that the strength of the present composite obeys the Weibull distribution function to a first approximation. From the slope, the shape parameter m was estimated to be 8.9.

According to the Weibull distribution function, the relation between the specimen size and the strength is expressed by

$$\frac{\sigma_2}{\sigma_1} = \left(\frac{V_1}{V_2}\right)^{1/m} \tag{1}$$

*Model JST-T220, Jeol-Technics Co., Ltd., Tokyo, Japan.

where V_1 and V_2 are the volumes of the gage part in the 8 mm- and 40 mm-width specimens, respectively, and σ_1 and σ_2 are the average strengths for the 8 mm- and 40 mm-width specimens, respectively. Substituting $\sigma_1 = 145$ MPa, $V_1 = 560\ \text{mm}^3$ (thickness: 2 mm, width: 8 mm, gage length: 35 mm), $V_2 = 7200\ \text{mm}^3$ (thickness: 2 mm, width: 40 mm, gage length: 90 mm) and $m = 8.9$ into Equation 1, we have $\sigma_2 = 109$ MPa. The calculated value of 109 MPa was in fairly good agreement with the experimentally measured value of 119 MPa. From this result, the difference in strength between 8 mm- and 40 mm-width specimens can be attributed mainly to the difference in effective volume.

Interfacial debonding and pull-out of fiber were remarkably observed in the fracture surface of all specimens, as typically shown in Fig. 4. Such features could be attributed to the low interfacial strength low due to the existent carbon layer on fiber surface which formed during processing (Fig. 1b), as confirmed in our former work [8].

3.2. Fracture behavior of notched specimen

Figs 5 and 6 show the relation between gross fracture strength σ_g and relative notch length $2a/W$ of the 8 mm- and 40 mm-width specimens, respectively. The strength at $2a/W = 0$ corresponds to the unnotched one.

In the case of the net stress criterion, the relation between gross fracture strength σ_g and relative notch length $2a/W$ is expressed by

$$\sigma_g = \sigma_f(1-\alpha) \quad (\alpha = 2a/W) \tag{2}$$

where σ_f is the tensile strength of unnotched specimen, $2a$ is the double edge notched length and W is the specimen width. Substituting $\sigma_f = 145$ and 119 MPa for 8- and 40 mm-width specimens, respectively, into Equation 2, we have the relation of σ_g to $2a/W$ based on the net stress criterion as shown with the solid lines in Figs 5 and 6. It is noted here that the difference in strength between room temperature and 1400°C, which could be attributed to the softened matrix (SiO_2 with dispersed TiC particle in this composite) at 1400°C [9, 10], is small.

In the case of fracture toughness criterion, the relation between gross fracture strength σ_g and relative notch length $2a/W$ is expressed by

$$\sigma_g = \frac{K_{IC}}{\sqrt{\frac{\pi W}{2}}\sqrt{\alpha}\, f(\alpha)} \tag{3}$$

$$f(\alpha) = 1.122 - 0.154\alpha + 0.807\alpha^2 - 1.894\alpha^3 + 2.494\alpha^4 \tag{4}$$

where K_{IC} is the fracture toughness for mode I [14]. Substituting the assumed values of $K_{IC} = 6, 8$ and 10 MPa$\sqrt{m}$ into Equation 3, we have the $\sigma_g - 2a/W$ relation based on fracture toughness criterion as shown with the dotted curves in Figs 5 and 6, for 8 and 40 mm widths, respectively. As shown in Fig. 5, the fracture strength of the notched 8 mm-width specimen at room

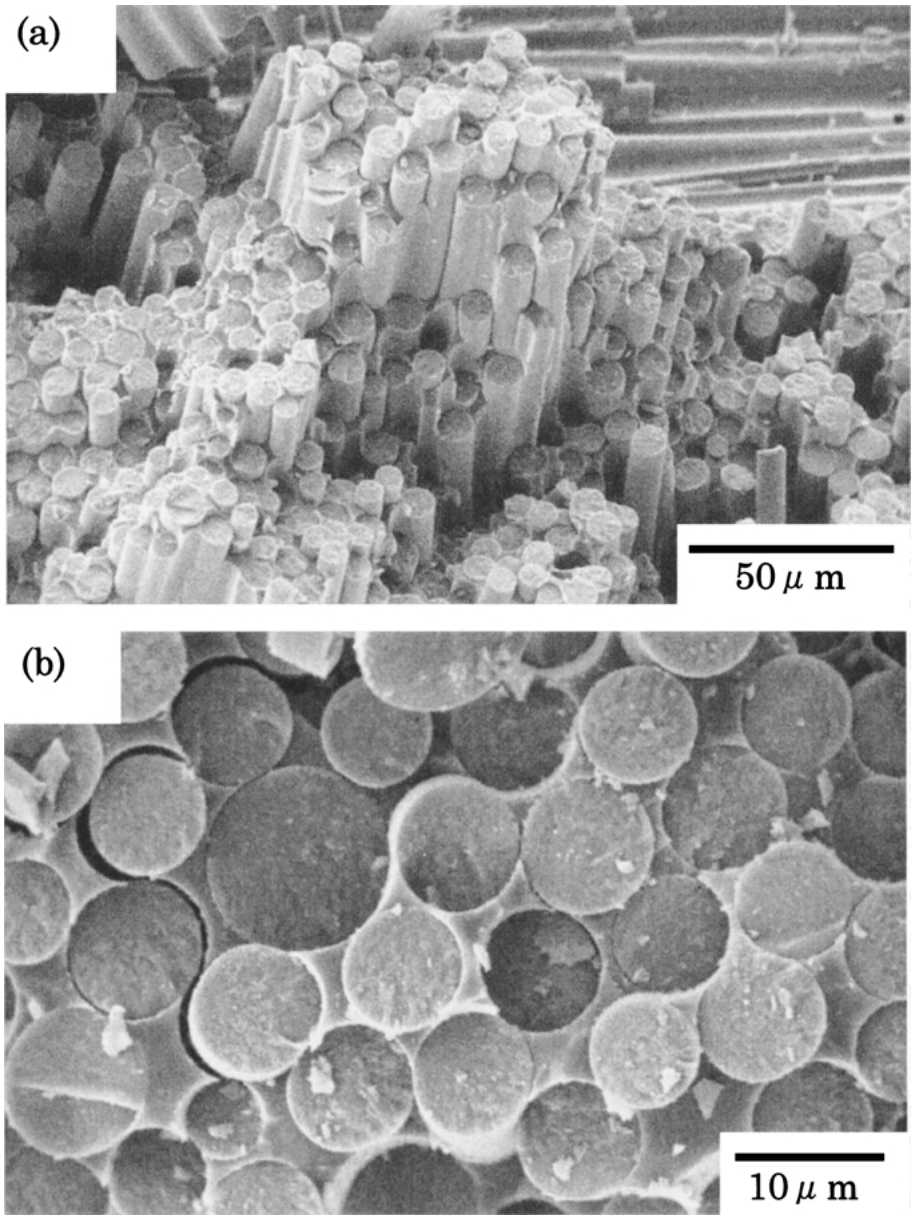

Figure 4 Typical fracture morphology of unnotched specimen with 8 mm width.

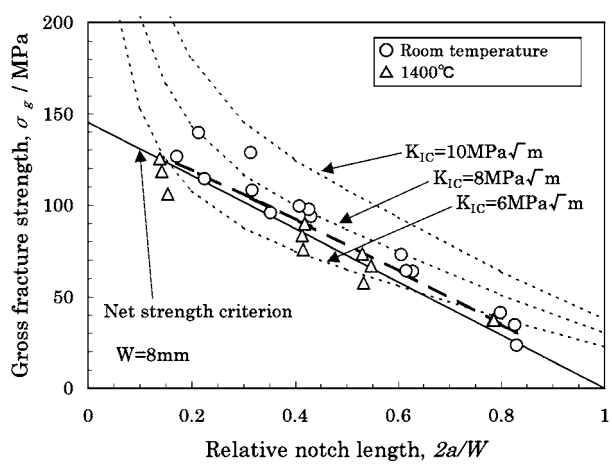

Figure 5 Relation between the gross fracture strength σ_g and the relative notch length $2a/W$ of the 8 mm-width specimen. The solid line show the relation of σ_g to $2a/W$ based on the net stress criterion. The broken line shows the relation of σ_g to $2a/W$ based on the net stress criterion in which the effective volume dependence of the ligament strength is incorporated. The dotted curves show the relation of σ_g to $2a/W$ based on the fracture toughness criterion.

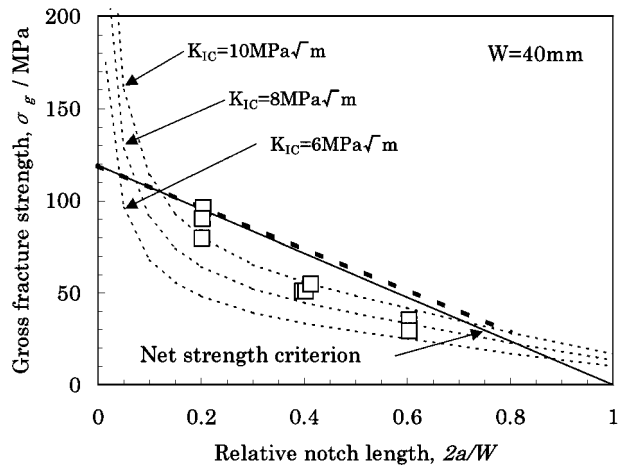

Figure 6 Relation between the gross fracture strength σ_g and the relative notch length $2a/W$ of the 40 mm-width specimen. The solid line show the relation of σ_g to $2a/W$ based on the net stress criterion. The broken line show the relation of σ_g to $2a/W$ based on the net stress criterion in which the effective volume dependence of the ligament strength is incorporated. The dotted curves show the relation of σ_g to $2a/W$ based on the fracture toughness criterion.

temperature was described fairly well by the net stress criterion. This result indicates that this composite is not sensitive to the notch and can be used safely from room temperature to high temperature when the width is narrow as 8 mm. On the other hand, the fracture strength of notched specimens with a 40 mm width at room temperature showed a slight shift from the net stress criterion toward the fracture toughness criterion for $K_{IC} = 10$ MPa$\sqrt{m}$ (see in Fig. 6).

If we assume that the net stress criterion is applicable to both 8 and 40 mm-width specimens and the strength of the ligament obeys the Weibull distribution, the strength of the ligament is expected to increase with increasing $2a/W$, since the volume of the ligament decreases. To examine it, the strength of the ligament (σ_{lig}) of each notched specimen was calculated by substituting the measured gross fracture strength σ_g and corresponding $2a/W$ into Equation 2. For convenience, the calculated value of σ_f was normalized with respect to the unnotched strength σ_f (145 and 119 MPa for 8 and 40 mm width-specimens, respectively). The plot of the normalized values of σ_{lig}/σ_f against $2a/W$ is shown in Fig. 7. Following features are read from Fig. 7.

(1) The σ_{lig}/σ_f value of 8 mm-width specimen increased slightly with increasing relative notch length, indicating that the strength of the ligament increased with decreasing effective volume. Under the Weibull distribution, the ligament strength increases with $2a/W$ through the volume effect expressed by $(1-2a/W)^{1/m}$ ($m = 8.9$ in the present specimens), as shown with the solid curve in Fig. 7. The measured variation of the strength of the ligament is fairly well described. When the effective volume dependence of ligament strength is incorporated, the $\sigma_g - 2a/W$ relation is calculated as shown with the broken lines in Figs 5 and 6, which are not so much different from the solid lines, also indicating that the net stress criterion is applicable to 8 mm-width specimens but not to 40 mm-width ones.

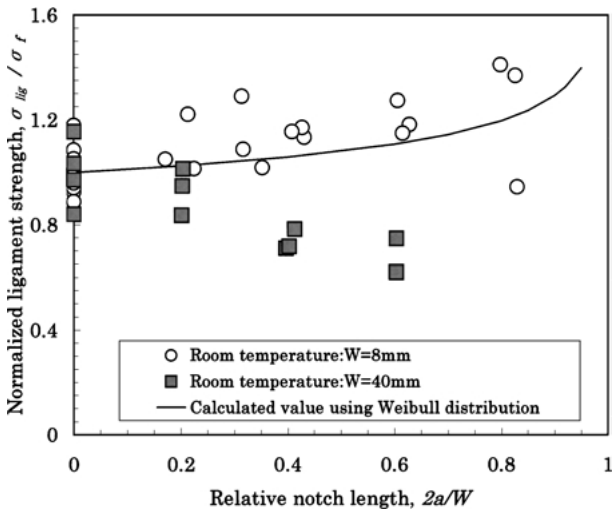

Figure 7 Relation between the ligament strength σ_{lig} normalized with respect to the unnotched strength σ_f (145 and 119 MPa for 8 and 40 mm width-specimens, respectively) and relative notch length $2a/W$.

(2) On the other hand, the strength of the ligament of the 40 mm-width specimens tends to remain up to $2a/W = 0.2$ but tends to decrease with increasing relative notch length when $2a/W$ is high as 0.4 and 0.6. The tendency at high $2a/W$ for 40 mm-width is opposite for 8 mm-width specimen. This means that the fracture of 40 mm-width specimens for $2a/W > 0.2$ cannot be described by the net stress criterion in contrast to that of 8 mm-width ones. Also it means that the strength-raising effect by the decrease in effective volume at high $2a/W$ is hindered in the 40 mm-width specimens. The reason for this is discussed below.

3.3. Fracture morphology of notched specimen

For all test temperatures, specimen width and relative notch length, similar fracture morphology was observed; namely the transverse fiber strands were broken perpendicular to tensile axis and the fibers in the longitudinal strands showed pull-out. The fracture surface of the notched 40 mm width specimen with $2a/W = 0.4$ is representatively presented in Fig. 8. From the fracture surface of all specimens, the pull-out length of fiber was measured. The result is shown in Fig. 9. The average pull-out length was irrelevant to the notch length, test temperature and specimen width, while the scatter was large. The average pull-out length was around 0.4 mm.

As stated above, there is a tendency that the fracture criterion shifts from the net stress criterion to fracture toughness criterion with increasing specimen width in the present composite. Similar result has been observed also for plain-woven C/C composite [11], where it was emphasized that the geometry of fiber strands in the weave affects on the formation of the damage zone. Here also the relation of the geometry to fracture strength is studied. Fig. 10 shows the geometry of the

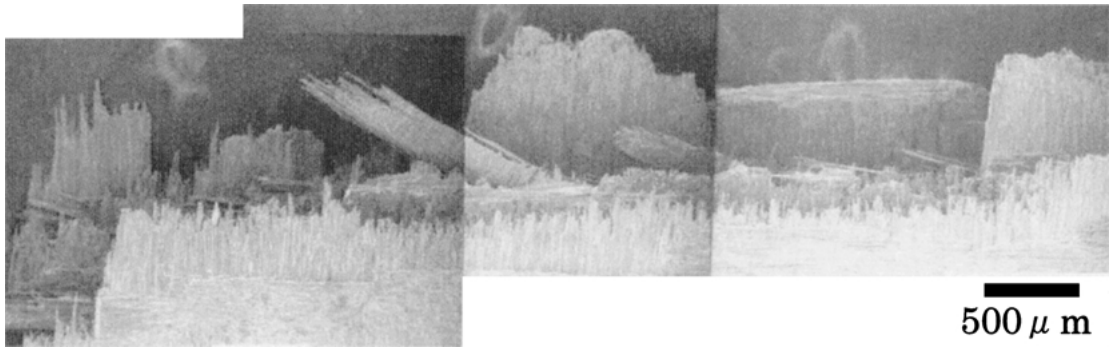

Figure 8 Fracture morphology of notched 8 mm-width specimen with $2a/W = 0.4$.

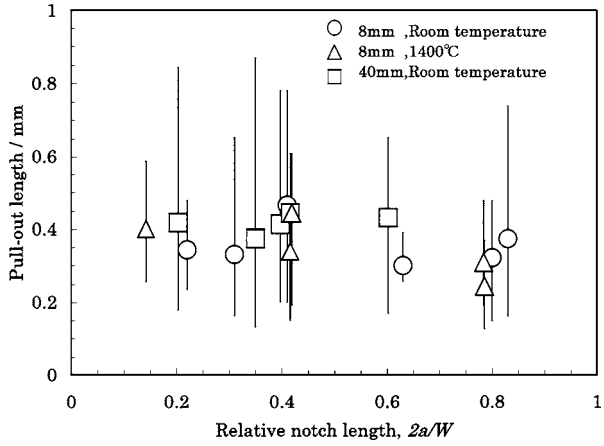

Figure 9 Relation between the relative notch length $2a/W$ and the pull-out length of fiber measured from the fracture surface.

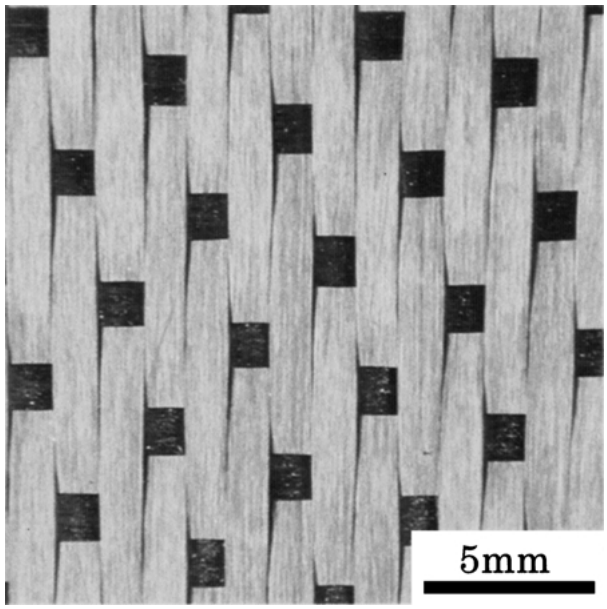

Figure 10 Photograph showing the geometry of the present satin woven fabric. The black and white parts correspond to the transverse and longitudinal directions of fiber, respectively.

present satin woven fabric. The black and white parts correspond to the longitudinal and transverse directions of fiber, respectively. Consequently, the back site surface of this woven fabric has the morphology with the 90 degree-rotated fiber. Fig. 11 shows the schematic drawing of the fabric, taken from the geometry in Fig. 10. The fiber strands of the longitudinal and transverse directions are numbered as X1 to X8 and Y1 to Y8, respectively. The present eight-harness satin weave fabric is composed of the repeated unit shown by the dotted region. The longitudinal strands are periodically constricted by the transverse ones and vice versa. Thus, the part with and without constriction exists periodically. Taking the case of constriction of X1 to X8 longitudinal strands by the Y1 transverse strand as an example, X1 is constricted but not X2 to X8. If we take the case of constriction of X1 to X8 by Y2, X4 is constricted but not X1 to X3 and X5 to X8. In this way, the transverse distance without constriction (=distance between X2 to X8 in the former case, which is the same as the distance between X4 in the present and the neighboring

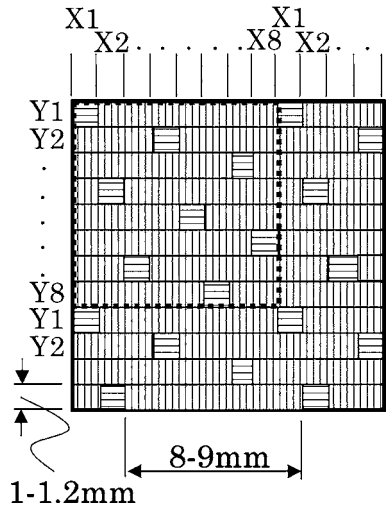

Figure 11 Schematic drawing of the fabric, taken from the geometry in Fig. 10.

units in the latter case) was estimated to be 8–9 mm, as shown in Fig. 11. The longitudinal length of each transverse strand (Y1, Y2...) was 1–1.2 mm, as also shown in Fig. 11.

The former value of 8–9 mm is near to the notch length 8 mm at which the fracture criterion shifted from the net stress criterion toward the fracture toughness one in the 40 mm width specimens. This implies that, when the notch length exceeds the periodical spacing 8-9 mm, the stress distribution ahead of the notch tends to be similar to that calculated by the linear fracture mechanics and thus the fracture behavior is correlated to the fabric geometry. Such a feature is similar to that observed for plain-woven C/C composite [11] on the point that the periodical spacing plays the dominant role in size-dependent fracture behavior of woven composites. Within the range of the present work, the empirical correlation between fracture criterion and fabric geometry was suggested in a qualitative manner. Further study is needed to clarify the mechanism quantitatively.

It is emphasized here that the latter value of 1–1.2 mm is near to the total pull-out length (0.8 mm on an average) in upper and lower fracture surfaces. This suggests that the fracture of fiber occur mainly within this length due to the constriction of the longitudinal fiber strands by the transverse fiber strands.

4. Conclusion

Fracture behavior of Si-Ti-C-O fiber-bonded ceramic produced by hot-pressing an oxidized satin-woven Si-Ti-C-O fiber was examined by using unnotched and double edge notched tension test specimens with different width (8 and 40 mm). Tensile strength of the unnotched specimens for 8 mm width was higher than that for 40 mm width. The specimen size-dependence of unnotched strength could be described quantitatively from the viewpoint of difference in effective volume by application of the measured Weibull's shape parameter. The strength of the notched specimen with 8 mm width at room temperature and 1400°C was described fairly well by the net section stress criterion. The strength for

40 mm width at room temperature, however, shifted from the net stress criterion toward the fracture toughness criterion, when the notch length was longer than 8 mm. The fracture strength of the specimen with notch less than 8 mm in length tends to obey the net stress criterion. The pull-out length and the applicability of the net stress and fracture toughness criteria are correlated to the fabric geometry. The present result can be utilized for the safety design on application of the composite as thermostructural parts.

References

1. C. F. WINDISCH JR., C. H. HENAGER JR., G. D. SPRINGER and R. H. JONES, *J. Amer. Ceram. Soc.* **80**(3) (1997) 567.
2. H. WANG and R. N. SINGH, *J. Mater. Sci.* **32** (1997) 3305.
3. M. G. JENKINS and M. D. MELLO, *Materials and Manufacturing Processes* **11**(1) (1996) 99.
4. T. ISHIKAWA, S. KAJII, Y. KOHTOKU and T. YAMAMURA, *Ceramic Engineering and Science Proceedings* **18**(3) (1997) 771.
5. T. ISHIKAWA, S. KAJII, K. MATSUNAGA, T. HOGAMI and Y. KOHTOKU, *J. Mater. Sci.* **30** (1995) 6218.
6. K. MATSUNAGA, T. ISHIKAWA, S. KAJII, T. HOGAMI and Y. KOHTOKU, *ibid.* **36** (2001) 1665.
7. S. KAJII, T. ISHIKAWA, K. MATSUNAGA and Y. KOHTOKU, *Advanced Performance Materials* **1** (1994) 145.
8. K. MATSUNAGA, T. ISHIKAWA, S. KAJII, T. HOGAMI and Y. KOHTOKU, *J. Ceram. Sci. Japan Int. Edition* **103** (1995) 292.
9. *Idem., J. Japan Inst. Metals* **60**(12) (1996) 1236.
10. *Idem., J. Mater. Sci.* **34** (1999) 1505.
11. M. YATOMI, M. HOJO, M. TANAKA, S. OCHIAI and J. TAKAHASHI, *J. Soc. Mat. Sci., Japan* **47**(9) (1998) 939.
12. M. TANAKA, S. OCHIAI, M. HOJO, T. ISHIKAWA, S. KAJII, K. MATSUNAGA and T. YAMAMURA, *Key Engineering Materials* **164/165** (1999) 141.
13. W. WEIBULL, *J. Appl. Mech.* **18** (1951) 293.
14. Y. MURAKAMI, S. AOKI, N. HASEBE, Y. ITOH, H. MIYATA, N. MIYAZAKI, H. TERADA, K. TOHGO, M. TOYA and R. YUUKI, "Stress Intensity Factors Handbook Vol. 1," Pergamon Press, 1987 p. 6.

Received 6 January
and accepted 29 November 2001